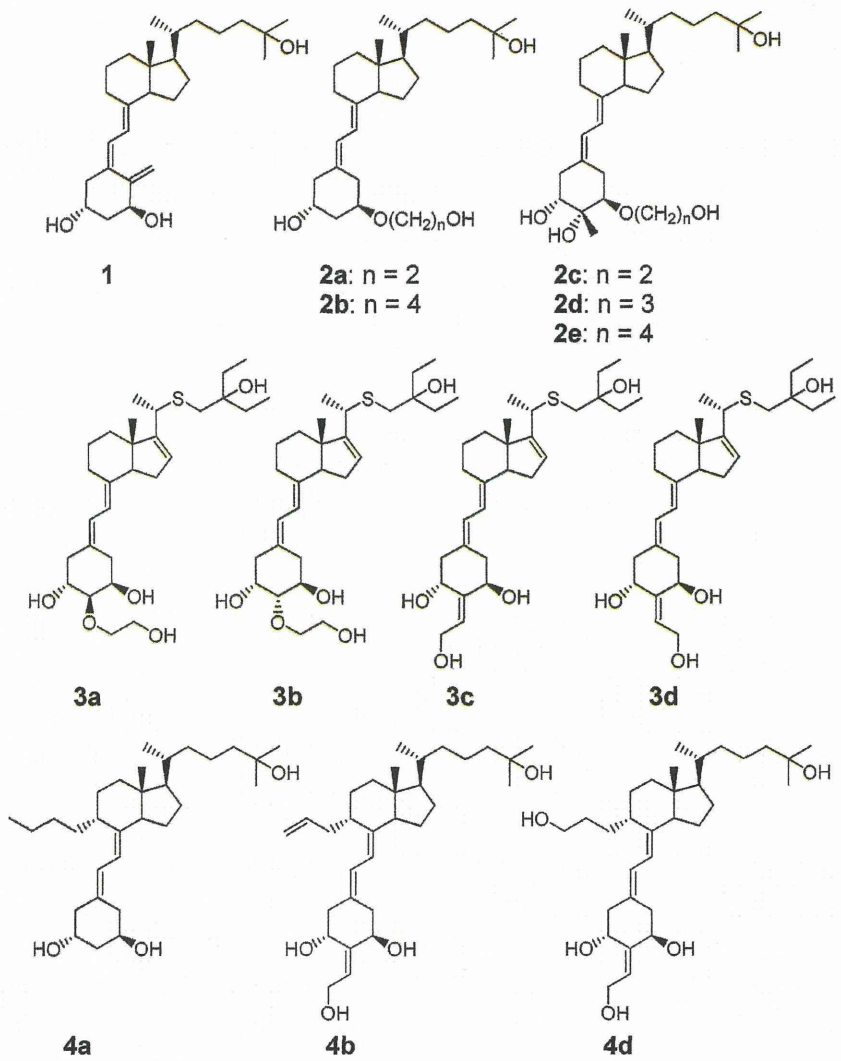

Figure 1. Structures of the vitamin D analogues discussed in this article.

rescue the functions disrupted by the missense mutations in the VDR-LBD.

Fifteen missense mutations have been identified in the LBD[7b] that reduce or abolish VDR functions, such as ligand binding and ligand-dependent transactivation. So far, only the crystal structure of the HVDRR H305Q mutant has been reported.[8] The H305Q mutation causes a 10-fold reduction in $1,25(OH)_2D_3$-dependent transactivation, and patients with this mutation can be treated with the natural hormone. The missense mutation R274L,[9] however, causes a >1000-fold reduction in responsiveness to the natural hormone. Patients with this mutation are hardly responsive to treatment with $1,25(OH)_2D_3$. Another severe mutation is W286R.[10] Patients with this mutation never respond to the natural hormone.

Here, we present the crystal structures of rat (r) VDR-LBD R270L and W282R mutants, which correspond to the human (h) R274L and W286R VDR mutants, respectively. We also designed and synthesized several ligands (**2a–e**, **3a–d**, and **4a–e**) (Figure 1) for use with these mutants. On the basis of these crystal structures and results of in vitro biological assays with ligands (**2a–e**, **3a–d** and **4a–e**), we discuss how these mutations disrupt the VDR function. Our data also provide clues for the design of novel therapeutic compounds for the treatment of HVDRR patients. Thermal unfolding experiments and CD spectral analysis also provided data that could not be obtained from the X-ray analysis alone to characterize these mutants.

RESULTS

Crystal Structures. We crystallized the rat VDR-LBD with a deletion mutation (rVDR-LBD 116–423, Δ165–211) in the long loop between helices H2 and H3[11] because it readily provided high quality crystals even with the point mutations. Human and rat VDRs share 89.5% identity overall and are 97.2% identical within the ligand-binding pocket (LBP). Therefore, crystal structures of rVDR-LBD mutants also provide important structural information about hVDR-LBD mutants. From this point in this article, rVDR-LBD (Δ165–211) will be referred to as WT, and its substitution mutants will be referred to as R270L and W282R, respectively.

The crystals of WT, R270L, and W282R were grown in the presence of the natural hormone (**1**) or one of the ligands

dx.doi.org/10.1021/jm400537h | J. Med. Chem. 2013, 56, 6745–6760

designed for the mutants (**3c** and **3d** for R270L, **4a** and **4b** for W282R; Figure 1) and with a peptide containing the LXXLL motif derived from the coactivator DRIP205 (MED1).[12] This peptide, which is essential for crystallizations, not only stabilizes the crystals by binding to the surface between the termini of the helices H3 and H12, known as the coactivator recognition surface (the AF-2 surface), but also participates in crystal packing (Figure S1, Supporting Information).

All of the crystals belonged to the same space group *C*2 as other rVDR complexes do.[11,13] The R270L complexes with ligands **1**, **3c**, and **3d** were refined to resolutions of 1.70, 1.90, and 2.11 Å (PDB ID: 3VT3, 3VT4, and 3VT5, respectively). The WT complex with ligand **3c** was refined to a resolution of 2.30 Å (PDB ID: 3VT6). The W282R complexes with ligands **1**, **4a**, and **4b** were refined to resolutions of 1.65, 2.10, and 2.35 Å (PDB ID: 3VT7, 3VT8, and 3VT9, respectively). Summaries of data collection and refinement statistics are shown in Tables S1, S2, and S3 (Supporting Information).

The overall folds of the VDR-LBDs in these complexes were fundamentally identical to those of the known h- and rVDR-LBD complexes with the natural hormone,[11a,14] as well as its agonistic[13c,15] and antagonistic analogues.[11b,13a,b,d] All seven complexes adopted the canonical active conformation of the VDR-LBD, and the coactivator peptide bound to the AF-2 surface. The root-mean-square deviations (rmsd) of the equivalent Cα atoms of the mutants (R270L and W282R) complexed with 1,25$(OH)_2D_3$ and the synthetic ligands (**3c**, **3d**, **4a**, and **4b**) from the corresponding WT complex (PDB ID: 2ZLC) were 0.15 to 0.30 Å. For comparison, we used rVDR-LBD (2ZLC) reported by us[16] but not that (1RK3) reported by Vanhooke's group[11a] because the conditions we used to prepare the crystals were nearly identical to those used for 2ZLC. The difference in the crystallization conditions used caused some changes in the loop region structures (rmsd, 0.4–0.9 Å). In calculating Cα rmsds, we eliminated the terminal atoms that had large rmsds values of >1.00.

R270L Complexed with the Natural Hormone 1,25-$(OH)_2D_3$. We successfully crystallized R270L complexed with 1,25$(OH)_2D_3$ in its active ternary complex as evidenced by the corresponding density clearly seen in the $2F_{obs} - F_{calc}$ map (Figure S2, Supporting Information). The Cα structure was nearly identical to that of WT (2ZLC), as indicated by the total rmsd (0.15 Å). The Cα positions shifted slightly near the mutation, Leu269 (0.45 Å) and Met268 (0.30 Å). Two water molecules are found in the space created by the mutation of arginine to leucine (Figure 2A); one of these water molecules forms a hydrogen bond with the 1α-OH group, and the other forms a hydrogen bond with the main chain carbonyl group of Thr142. These interactions, however, must be weak because the human R274L mutant showed a greater than 1000-fold reduction in transcriptional responsiveness to the natural hormone.[9] In the WT, Arg270 formed direct hydrogen bonds with the 1α-OH group and the main chain carbonyl of Thr142. These direct interactions might be important to keep the conformation of the loop 1–2 and for the function of the VDR. Ligand recognition by the mutant, otherwise, is very similar to that of the WT, that is, 1,25$(OH)_2D_3$ (**1**) is anchored by five hydrogen bonds.

R270L in Complex with Ligands 3c and 3d. Ligands **3c** and **3d** are super agonists for wild-type hVDR.[16] They were also good agonists for R274L hVDR, being 130 and 40 times, respectively, more potent than **1** (see below). The complexes of R270L with **3c** and **3d** adopt the same active conformation as

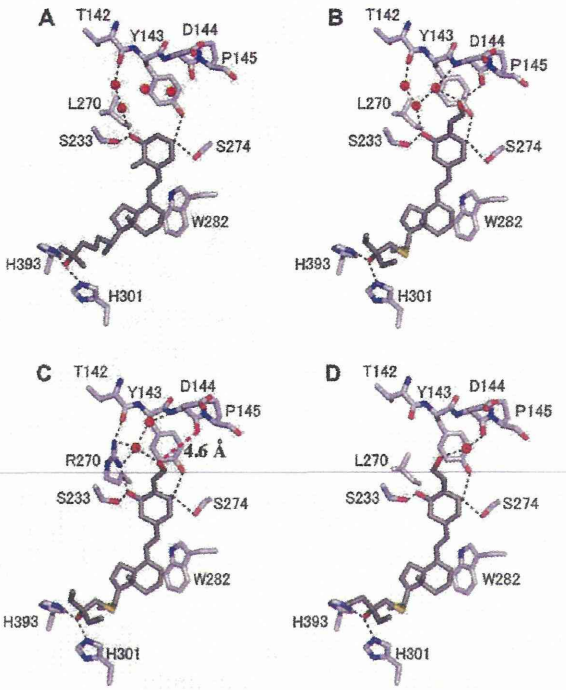

Figure 2. Hydrogen-bonding interactions in the complexes of R270L. (A) R270L with **1**, (B) R270L with **3c**, (C) WT with **3c**, and (D) R270L with **3d**. Black dotted lines show hydrogen bonds. Ligands (dark gray, carbon; red, oxygen; and yellow, sulfur) and protein residues (white, carbon; red, oxygen; and blue, nitrogen) are shown as sticks and water molecules as red balls. The magenta dotted line in C shows the distance between the terminal hydroxyl group of **3c** and the main chain carbonyl group of Asp144.

that of the WT. The Cα rmsds of R270L complexed with **3c** and **3d** from WT (2ZLC) were 0.23 and 0.19 Å, respectively.

In the complex of R270L with **3c**, the terminal hydroxyl group of the substituent at C(2) directly interacts with the main chain carbonyl group of Asp144 (Figure 2B). This interaction replaced the lost direct interactions among the 1α-OH group of the ligand, Arg270, and Thr142 and explain why **3c** was 130 times more active than **1** for hR274L. The defective interaction with L270 made the ligand slightly move to Asp144 to form the hydrogen bond. In the complex with WT (Figure 2C), the terminal hydroxyl group of **3c** was 4.6 Å away from the carbonyl group of Asp144. Compound **3c** also interacted with Thr142 via two water molecules (Figure 2B). Because of these interactions, the Cα positional shifts of Thr142, Asp144, and Pro145 from those of the WT/1,25$(OH)_2D_3$ complex were somewhat large at 0.40, 0.55, and 0.63 Å, respectively. These changes might affect the conformation of Gln273 (positional shift, 0.48 Å) and Ser274 (0.48 Å) in the H5. Other than this difference, **3c**'s interaction with R270L was essentially identical to that with WT.

In the complex with R270L, **3d** does not directly hydrogen bond with Asp144, but it does hydrogen bond with a water molecule that, in turn, interacted with Asp144 (Figure 2D). This difference explains the difference in the activity of **3d** compared with **3c**.

W282R with Several Ligands. Trp286 in the hVDR-LBD (Trp282 in rVDR-LBD) interacts strongly with the vitamin D ligand.[11a,14] The interactions occur at its 2-, 3a-, 4-, and 7a-

dx.doi.org/10.1021/jm400537h | J. Med. Chem. 2013, 56, 6745–6760

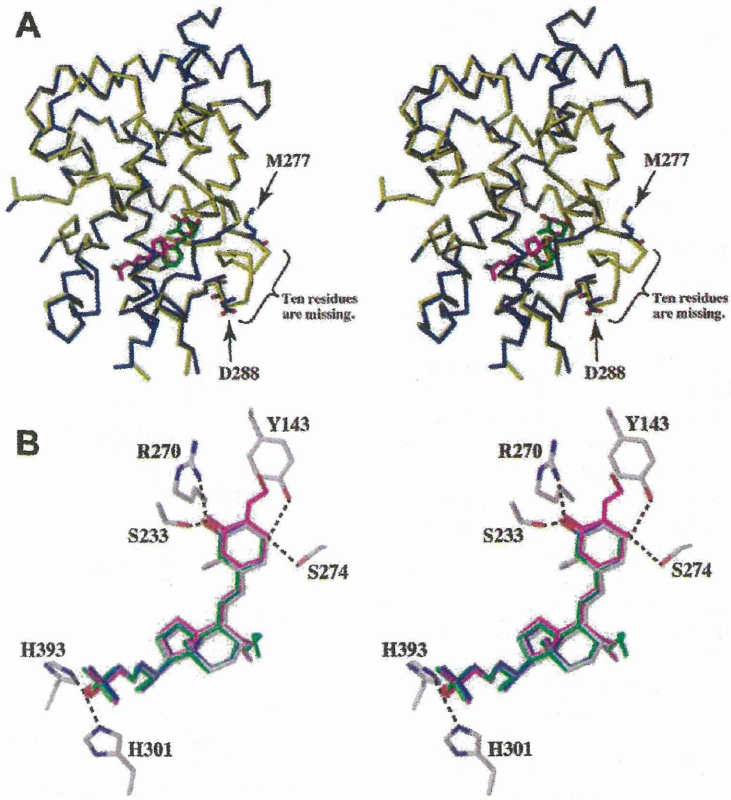

Figure 3. Overlays of the crystal structures of W282R and WT (stereoviews). (A) Overlay of the Cα structures of W282R and WT in complex with 1,25$(OH)_2D_3$ (WT, yellow protein with green ligand; W282R, blue protein with magenta ligand). The W282R structure lacks 10 residues from Asp278 to Gln287. (B) Overlay of the ligands in WT (2ZLC) (atom type) and in W282R (**1**, **4a**, and **4b**; blue, green, and magenta, respectively) and the hydrogen-bonding residues in 2ZLC. The dotted lines show hydrogen bonds.

positions with the 6-, 8-, and 9-positions of the ligand over distances of less than 4 Å (Figure S3A, Supporting Information). The Trp286 also interacts with Phe279, Gln317, Tyr295, Ser275, Ser278, Leu313, and Ile314. As a result, its mutation to Arg abolishes the activity of the VDR mutant.[10]

We succeessfully crystallized ternary complexes of the W282R mutant with the natural hormone and two synthetic ligands (**4a** and **4b**), and the coactivator-derived peptide. The 9α-substituted ligands (**4a** and **4b**) were designed on the basis of the model of the mutants. The substituent at the 9α-position was directed toward Trp282 and expected to occupy the space yielded by the Trp to Arg mutation (Figures S3B and S4C, Supporting Information).

W282R in Complex with the Natural Hormone. The crystal structure of W282R in complex with the natural hormone was determined as the canonical active conformation (Figure 3A). Surprisingly, a group of residues neighboring of Arg282 were not visible in the electron density map of the mutant complex with the natural hormone (Figures 4A and B), suggesting that these residues were highly disordered. We did not observe any interpretable density in the W282R structure for 10 residues between Asp278 and Gln287 (Figure 4A). This disorder at the β-strand part affected the conformation of the beginning of loop 1−2, from Pro145 to Ala148 (positional shift, 0.35−0.79 Å). Yet, despite such a drastic disorder in the secondary structure, the overall folds of the mutant remain nearly identical to those of the WT (rmsd 0.27 Å) (Figure 3A). We assume that the coactivator peptide trapped the active conformation of the mutant by binding to the AF-2 surface, which formed temporally when the mutant bound the ligand. Thus, the seemingly minor conformation of W282R in biological solutions was crystallized out under our crystallization conditions. Surprisingly, the ligand forms normal hydrogen bonds via its three hydroxyl groups (Figure 3B).

W282R with 9-Substitued Vitamin D Analogues (4a and 4b). The complexes of W282R with **4a** and **4b** exhibited similar disorder near the antiparallel β-sheet; the seven residues from Asp279 to Gly285 were not visible. In addition, the ligands themselves had high temperature factors at the terminal of the 9-substituent groups. For example, in the complex of W282R with **4a** or **4b**, the terminal atom of the 9-substituent had an especially high value of more than 45 Å^2 (Figures S3C and D, Supporting Information). Thus, the terminal atoms of the 9-substituents cannot be stabilized via interactions to receptor residues that are also disordered. However, both **4a** and **4b** form normal hydrogen bonds via their three hydroxyl groups (Figure 3B).

Ligand Additive Effects and Thermal Unfolding of rVDR-LBD Mutants Observed by Far-UV CD Spectra. To examine the thermal stability of the R270L and W282R mutants compared with WT, we monitored heat-induced unfolding transition experiments using CD spectra.[17] Equilibrium CD spectra were obtained in the far-UV regions at pH 7.0. The far-UV spectrum of a solution of ligand-free WT at 20 °C exhibited the typical spectrum of an α-helical structure, and

dx.doi.org/10.1021/jm400537h | J. Med. Chem. 2013, 56, 6745−6760

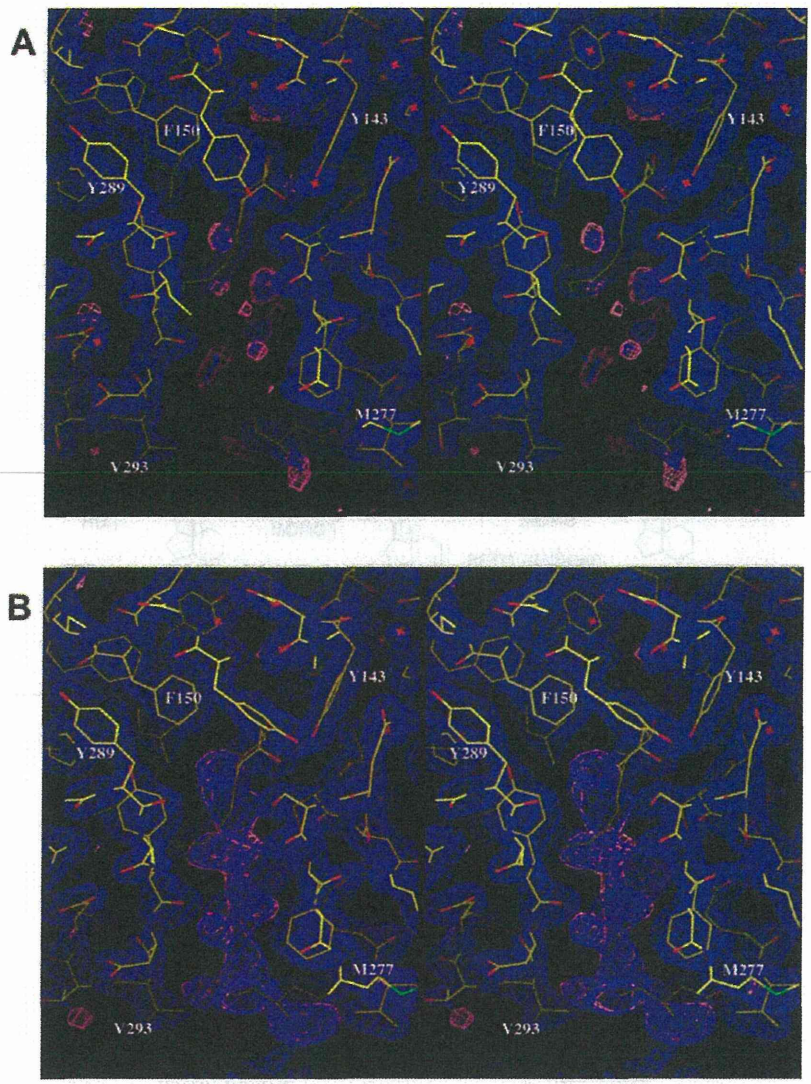

Figure 4. Electron density maps of W282R and WT complexes. (A) Electron density map of W282R/1,25$(OH)_2D_3$ around the β-sheet region (stereo view). (B) Electron density map of WT/1,25$(OH)_2D_3$ (PDB ID: 2ZLC) in the same region and orientation as that described above (stereo view). The $2F_{obs} - F_{calc}$ map (1.5 σ) is shown in blue, and the $F_{obs} - F_{calc}$ map (3 σ) is shown in pink. Notice that electron density around R282 (from Asp278 to Gln287) is missing in A but not in B.

the addition of the natural hormone confirmed this α-helical type spectrum[18] (Figure S5A, Supporting Information). R270L and W282R showed similar α-helical spectra to that of WT including the ligand-additive effect (Figures S5B and C, Supporting Information).

However, the three proteins WT, R270L, and W282R showed remarkable differences in their thermal stability. Figure S5D, E, and F (Supporting Information) shows the equilibrium transition curves at 222 nm of WT, R270L, and W282R, respectively, with and without the natural hormone. In the ligand-free solutions, the transition temperature (T_m) of WT was the highest (47.8 °C), whereas those of R270L and W282R were similarly lower (44.1 and 44.8 °C, respectively). In the presence of the natural ligand, the differences in the T_m values were more distinct. Ligand binding caused the T_m of WT to rise by 8.4 °C, whereas the T_m of R270L and W282R rose by only 2.5 and 0.1 °C, respectively. These results indicate that the ligand significantly stabilizes the WT but only weakly stabilizes R270L and has no stabilization effect on W282R. These results are consistent with the ligand binding behavior of the three proteins.

Synthesis of Agonists for Mutants R274L and W286R.

Agonist for R274L. Several studies have been reported to create specific agonist for mutants implicated in HVDRR. Swann et al.[19] reported that nonsecosteroidal ligands with a bisphenol scaffold showed potent transactivation for R274L. Kittaka et al. reported that vitamin D_3 analogues modified at the 1α-, 1β-, or 2α-position on the A-ring of vitamin D_3 improved the vitamin D action on the R274A and R274L mutants.[20]

We also designed and synthesized candidates of **2a**−**2e** and **3a**−**d** for hR274L (rR270L) (Figure 1). These candidates are 19-norvitamin D_3 analogues modified at the 1α-position (**2a** and **2b**), 1α- and 2-positions (**2c**−**2e**), and the side chain and 2-position (**3a**−**3d**).[16] Computer-aided molecular modeling

dx.doi.org/10.1021/jm400537h | J. Med. Chem. 2013, 56, 6745−6760

Scheme 1. Synthesis of Ligands 2a and 2b

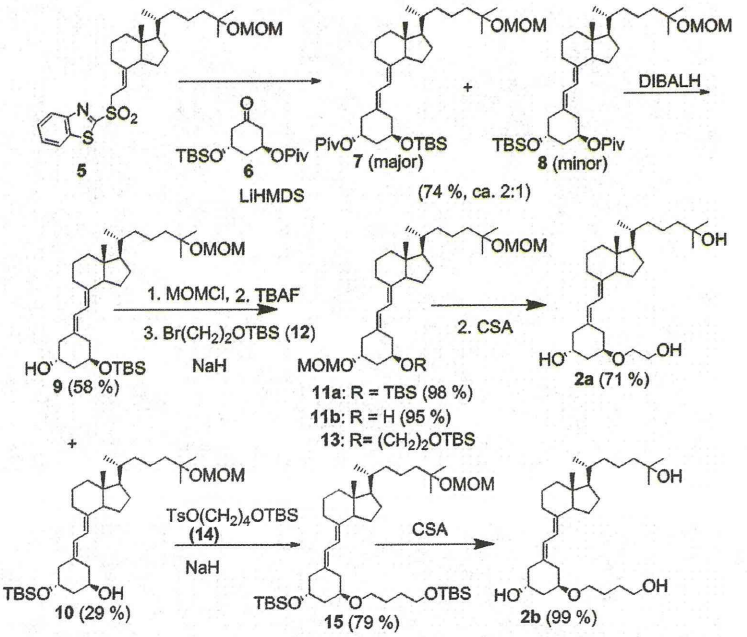

Scheme 2. Synthesis of Ligands 2c to 2e

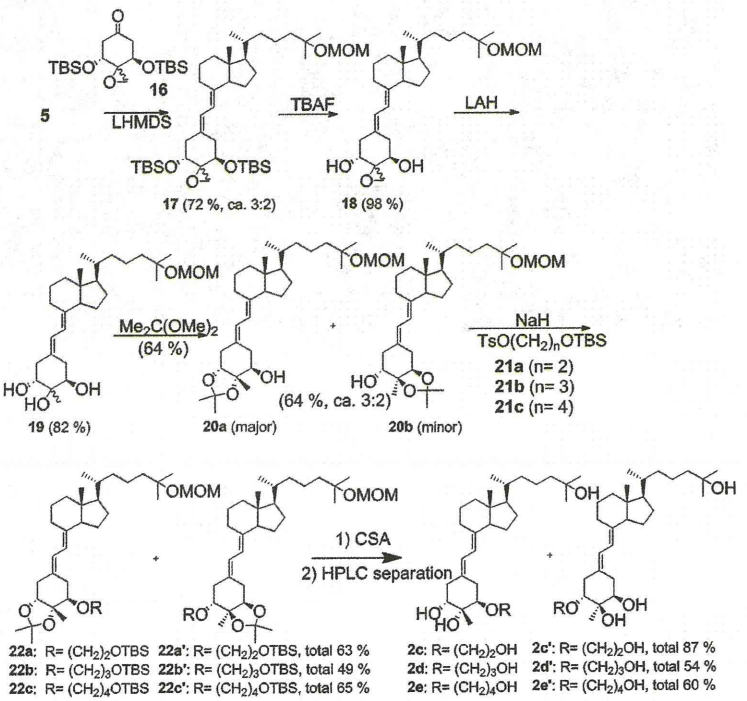

(Sybyl, Tripos) was used to design these ligands. The long substituent at the 1α-position was designed to fill the space newly generated by the Arg to Leu mutation (Figure S4A, Supporting Information). The 2α-methyl group of **2c**–**2e** was expected to interact with the hydrophobic residue above the A-ring and the 2β-hydroxyl group with the polar environment below the A ring.

The synthetic scheme of **2a** and **2b** is shown in Scheme 1. Julia-Kocienski reagent **5**[21] was coupled with A-ring fragment **6**, in which 1α- and 3β-hydroxyl groups were distinguished by protecting groups, to give 19-norvitamin D **7** and **8** as a 2:1 mixture (74%). After the pivaloyl group was removed (DIBALH), the free hydroxyl group of **9** was protected with the methoxymethyl (MOM) group (98%), and the *t*-butyldimethylsilyl (TBS) group was deprotected (95%) and

dx.doi.org/10.1021/jm400537h | J. Med. Chem. 2013, 56, 6745–6760

Scheme 3. Synthesis of Ligands 4a–4e

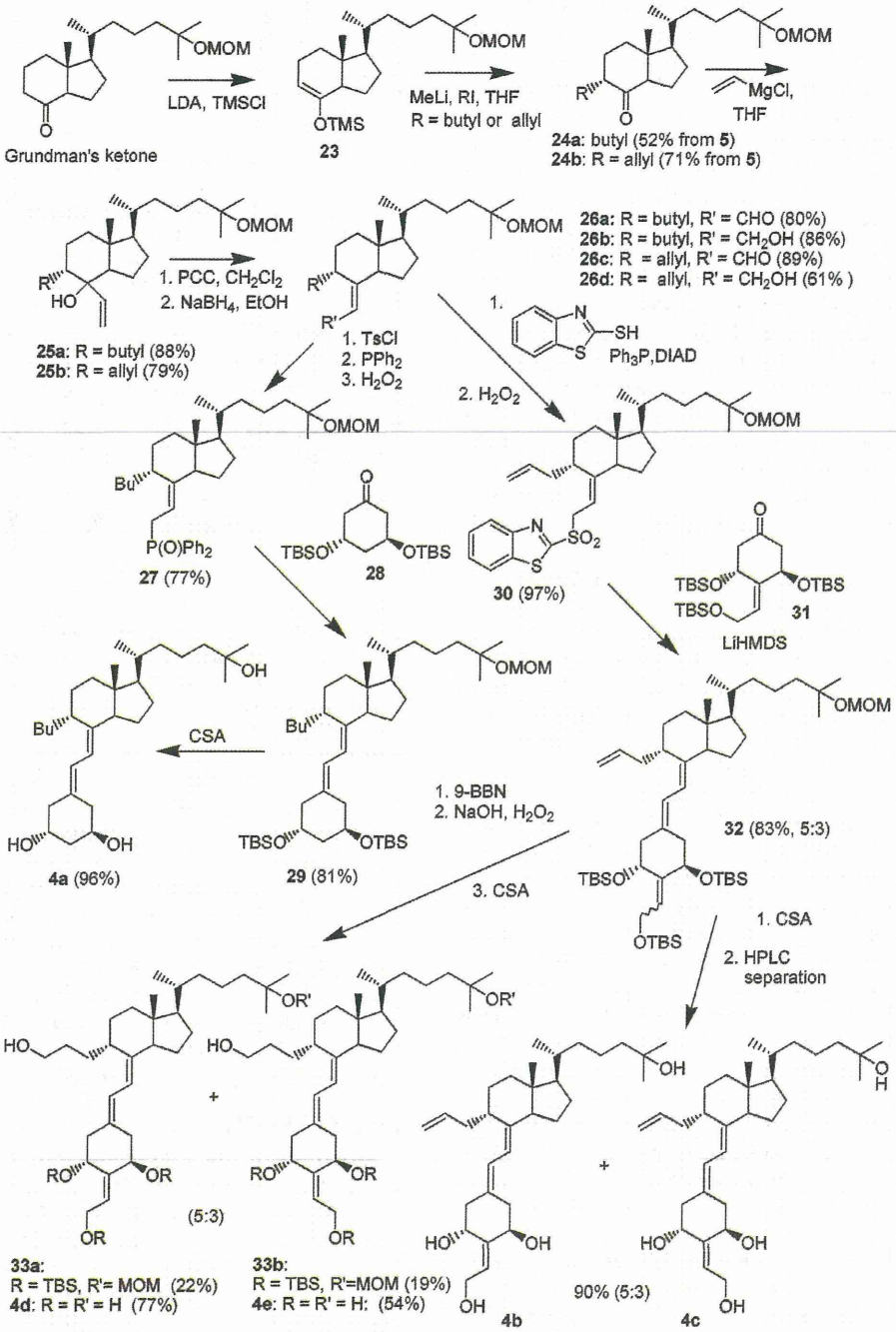

then treated with bromide **12** to give **13** (23%), the protecting groups of which were removed with camphor sulfonic acid (CSA) in MeOH to give 1α-hydroxyethoxy compound **2a** (71%). The hydroxy group of **10** was treated with tosylate **14** to give **15** (79%), the protecting groups of which were removed with CSA to give **2b** (99%).

The analogues **2c–e** were synthesized from **5** (Scheme 2). Compound **5** was treated with A-ring fragment **16** (72%), the TBS group was removed (98%), and the epoxide group was reduced with LAH to give triol **19** as an epimeric mixture at C(2) (82%). The *cis*-vicinal hydroxyl group of **19** was protected with 2,2-dimethoxypropane to give a 3:2 mixture of 2,3 (**20a**)- and 1,2-ketals (**20b**) (64%), and the remaining hydroxyl group was treated with tosylates **21a**, **21b**, and **21c** to give **22a**, **22b**, and **22c** (63%, 49%, and 65%), respectively. The protecting groups were removed with CSA, and then the products were separated by HPLC to give **2c**, **2d**, and **2e** and their regioisomers (total 87%, 54%, and 60%, respectively). The synthesis of **3a–d** was reported previously.[16]

Agonist for W286R. Using models of the W282R mutant, we hypothesized that a larger butyl group added to replace the 9α-hydrogen of vitamin D (Figure S3B, Supporting Information)

dx.doi.org/10.1021/jm400537h | J. Med. Chem. 2013, 56, 6745–6760

would fill the space formed upon substitution of the Trp to Arg (Figure S4C, Supporting Information). Thus, we synthesized vitamin D compounds substituted with a butyl (**4a**), allyl (**4b**), or 3-hydroxypropyl (**4d**) group at the 9α-position (Scheme 3).

Grundman's ketone was converted to enol trimethylsilyl ether (**23**), which was treated in situ with MeLi followed by butyl iodide or allyl iodide to give the 9α-substituted ketones **24a** or **24b** (71% or 52%, respectively). The ketones (**24a** and **24b**) were treated with vinyl magnesium chloride (**25a** 88% and **25b** 79%, respectively), oxidized with PCC to give aldehydes **26a** (80%) and **26c** (89%), respectively, which were then reduced to give alcohols **26b** (86%) and **26d** (61%), respectively. Compound **26b** was converted to Wittig reagent **27** (77%), combined with A-ring fragment **28** (21%, 74% based on the recovery of the starting material **27**), and deprotected with CSA to give **4a** (96%). The low yield of the Wittig–Horner reaction was probably due to the steric inhibition of the 9α-butyl group. For the synthesis of **4b–e**, we employed the Julia-Kociensky reaction to couple the A-ring and CD-ring fragments. Allyl alcohol **26d** was treated with 2-mercaptobenzothiazole in the presence of triphenyl phosphine and DIAD and then oxidized with H_2O_2 to give **30** (97%). Compound **30** was treated with A-ring fragment **31** to give **32** (57%, 83%, on the basis of the recovered **30**) as a 5:3 mixture of *E*- and *Z*-isomers at C(2), which were deprotected and separated by HPLC to give **4b** (2*E*-isomer) and **4c** (2*Z*-isomer) (5:3, 90% total). To obtain 9-hydroxypropyl compounds, **32** was allowed to undergo hydroboration followed by oxidation and deprotection to give **4d** (17% in three steps, 2*E*-isomer) and **4e** (10% in three steps, 2*Z*-isomer).

Biological Evaluation of Synthetic Ligands. *Ligands for R274L.* Ligands **2a** and **2b** were less active than the natural hormone in the luciferase assay with hR274L, and ligands **2c–e** have almost no potency (Figure 5A). Molecular modeling predicted a space that would be generated in the LBP by the mutation of Arg270 to Leu (Figure S4A, Supporting Information). However, the actual space in the LBP of R270L crystal structure differed slightly from the predicted space (Figure S4B, Supporting Information). The R270L had a pocket (Figure S4B, Supporting Information, yellow) that was narrower than we expected on the basis of the model (Figure S4B, Supporting Information, green), and accordingly, ligand **2b** did not fit correctly in the LBP of R270L. This difference was likely due to a slight movement of helix H5, which is difficult to predict by modeling. Therefore, the 1α-substituents of ligands **2a–e** were unable to enter the LBP due to steric congestion.

The ligands (**3a–3d**), which were initially designed as super agonists,[16] showed excellent activity for R274L: **3a**, **3b**, **3c**, and **3d** were 15, 4, 130, and 46 times more potent than **1** for R274L in transactivation (Figure 5B). Interestingly, while 2β-hydroxyethoxy-D analogue (**3b**) was the most potent for the WT VDR,[16] the 2*E*-hydroxyethylidene analogue (**3c**) appeared to be the most potent for the R274L mutant. Ligand **3c** had the highest activity for R274L because its terminal hydroxyl group directly interacted with the main chain carbonyl group of Asp144 (Figure 2B). Thus, **3c** may be a good candidate for the treatment of HVDRR caused by the R274L mutation.

Ligand **3d** was less active than **3c** for R274L because it interacted with Asp144 via a water molecule (Figure 2D). These results indicate that direct interactions are much stronger than indirect interactions via water.

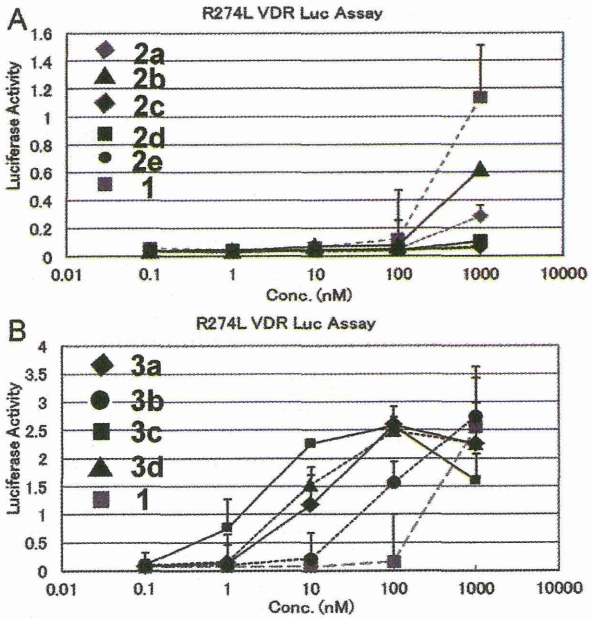

Figure 5. Transcriptional activities of **1** and synthetic ligands on R274L hVDR. The activities of **2a–e** and **1** (A) and **3a–d** and **1** (B) were evaluated by dual luciferase assay using a R274L full-length hVDR expression plasmid (pCMX-hVDR) and a luciferase reporter gene with a mouse osteopontin VDRE at the promoter (SPPx3-TK-Luc) in COS7 cells.

Ligands for W286R. Despite our design (Figures S3B and S4C, Supporting Information) and efforts, the 9-substitued compounds we synthesized had little to no potency on W286R hVDR (**4a** and **4c** to **4e**, data not shown; **4b**, see Figure S6, Supporting Information). The hydrophobic 9-substituent groups did not induce better folding of the disordered β-strands. The temperature factors shown on the ligand (Figure S3C and D, Supporting Information) suggest that shorter substituents would be better. Our findings also suggest that a negatively charged group introduced at the 9α-position may hold the Arg282 side chain inside the LBP, thereby maintaining the normal folding of the β-sheet part.

■ DISCUSSION

Structures of the R270L and W282R Mutant Proteins Would Be Trapped under Our Crystallization Conditions and Represent a Minor Population in Biological Solutions. Regardless of the mutants' low potency, the crystal structures of the ternary complexes of the mutant rVDRs adopted canonical active conformations. Because of the importance of the DRIP205 peptide in crystallization, it is clear that the peptide trapped the ligand-bound active conformation. Packing modes in the unit cell also supported crystallization of the active conformation (Figure S1, Supporting Information). In the most N-terminal part of the R270L complexed with the natural hormone (**1**), electron density of the residues of the expression tag sequence (Asn-Ser-Pro) was observed (Figure S1A and C, Supporting Information, red helix). These residues interact with Asp137 and His140 in the neighboring molecule in the crystal (Figure S1C, Supporting Information). In the crystal of W282R, the interactions of His130 with Glu304 and Glu307, and of Arg248 with Glu392 in the neighboring molecule were also

dx.doi.org/10.1021/jm400537h | J. Med. Chem. 2013, 56, 6745–6760

observed (Figure S1E, Supporting Information). These interactions between neighboring molecules were not observed in WT rVDR-LBD.

In contrast, thermal transition experiments in the solution state using CD spectra indicated that R270L was present in a nearly ligand-free and W282R completely ligand-free states, whereas WT was completely in the ligand-bound state. From all of these results, we concluded that these mutants R270L and W282R were crystallized as the complexes with ligands in the active conformations probably because the coactivator peptide binds to the AF-2 surface thereby stabilizing the complex. It is also clear that these mutants are free of the ligands in biological solution, as supported by the CD spectral analysis and by their biological activities.[9,10]

Substitution Mutation R270L Causes a Significant Change in the Main Chain Structure between Helices H1 and H2. The substitution mutation led to a local conformational change in the protein structure. A small difference (rmsd 0.13−0.28) in the coordinates of R270L/1,25$(OH)_2D_3$ compared with those of WT/1,25$(OH)_2D_3$ would be important. Arg274 in hVDR is essential for its interaction with the 1α-OH group of the ligand.[22] However, Arg274 also has an important interaction with the main chain carbonyl group of Thr142. The loop 1−2 of agonist-bound VDR-LBDs derived from humans, rats, and zebra fish, shares common secondary structural characteristics:[11a,14,15d] Glu126 to Thr142 displays a typical α-helix (H1), Thr142 to Pro145 forms a β-strand-like structure, Pro145 and Thr146 form a hydrogen-bonded turn, and Ala148 to Asp152 displays a 3_{10}-helix (H2). Thr142 and Tyr143 are particularly notable because they are tethered to the natural hormone. The Tyr143 side chain interacts directly with the 3β-OH of the ligand, and the Thr142 main chain carbonyl group interacts with Arg270, which interacts with the 1α-OH of the ligand. In the R270L mutant, Thr142 and 1α-OH are connected by interactions via two water molecules. Thus, one of the two interactions is weakened by the mutation. We previously performed a mutational analysis of all of the LBP residues of the VDR and reported that the single mutation of Y143A causes a marked reduction in ligand-dependent transactivation.[22,23] These results suggested that the local area structures between H1 and H2 influence ligand-dependent VDR functions. We confirmed in the present studies that water-mediated interactions are weaker than direct interactions between ligands and residues.

In the present study, the 2-substituted-19-norvitamin D_3 analogues **3a**, **3b**, **3c**, and **3d** showed potent agonistic activity against the hVDR R274L mutant (Figure 5B). Of these four derivatives, **3c** was the most effective agonist against the R274L mutant, whereas **3b** was the most effective against the WT VDR. We, therefore, suggest that **3c** is the most promising candidate among these analogues for the treatment of HVDRR caused by the R274L mutation.

Why Does the W286R Mutant Never Respond to Vitamin D Ligands? We also obtained the crystal structures of the W282R mutant as the ligand-bound active conformation. These structures would also represent a minor population in a biological solution because previous studies have shown that W286R hVDR never binds to the natural hormone and never responds to vitamin D-dependent gene transactivation.[10] However, the structures of these complexes have a notable feature. Ten to seven residues around the mutated part of the protein complexed with either 1,25$(OH)_2D_3$ or ligand **3a** or **3b** were not visible. Every VDR-LBD, including those of rats, humans, and zebra fish, has a set of antiparallel β-sheets. From the center of the β-sheet, Trp282 (or Trp286 in hVDR) protrudes to the seco-B and C ring parts of the ligand, where they strongly interact (Figure S3A, Supporting Information). In general, proteins favor hydrophobic residues on the inside and hydrophilic residues on the outside. Thus, unlike Trp, the hydrophilic Arg282 would favor the outside rather than the inside. This disruption of the β-strand conformation could lead to a partial unfolding of this part of the complex. We conclude that correct folding at the β-strand part is important for the VDR action. It has been reported[24] in the crystal structural study of intact peroxisome proliferator activating receptor γ (PPARγ)-RXRα complex on DNA that the β-sheet parts of the PPARγ form hydrophobic interactions with RXRα DBD and that these interactions can contribute to DNA recognition and affinity. The β-sheet part of the VDR may have similar function. A CD spectral study showed the stabilities of the WT, and the mutant widened drastically when the ligand was present. The mutation spoils the stability gain of the VDR upon ligand binding.

We designed the agonists (**4a**, **4b**, and **4d**) for the W286R mutant by paying attention to the position (C-9) of modification in the ligand. In future studies, we plan to examine the electronic compatibility of the ligand with the Arg side chain. For example, it would be interesting to introduce a negatively charged group at the 9α-position of the ligand.

CONCLUSIONS

We solved the crystal structures of two rVDR-LBD mutants implicated in HVDRR, R270L, and W282R, complexed with natural and synthetic vitamin D ligands and the coactivator DRIP205 peptide. All of the crystal structures adopted canonical active conformations. However, these active conformations are assumed to be minor conformations in biological solutions because the responsiveness of these mutants to the natural hormone are severely reduced or even eliminated. The binding of the coactivator peptide to the AF-2 surface may have facilitated the crystallization of the complex.

The mutations caused only local conformational changes. In R270L, we observed small Cα rmsd changes in the residues near the R270L mutation and the loss of direct interactions of Arg270 with the ligand and with Thr142. The hydroxyethylidene side chain at C(2) of analogue **3c** formed a hydrogen bond with Asp144 and restored the potency that was reduced by the mutation. We suggest that **3c** has potential as an agent for the treatment of HVDRR caused by the R274L mutation.

The W282R mutation disrupted the structure around the β-strands so that 7 to 10 residues around that position became invisible. This occurred probably because the Trp to Arg mutation changed the property of this portion from hydrophobic to hydrophilic. However, it should be noted that in the W282R/ligand complexes, all three hydroxyl groups of the ligands (**1**, **4a**, and **4b**) were doubly anchored by a pair of hydrogen bonds to the protein residues, suggesting that the six hydrogen bonds are not enough for the VDR in biological solution to anchor the ligands. Maintenance of the conformation around the β-strands is important for VDR function. We, therefore, suggest that vitamin D derivatives with a 9α-substituent that has a negative charge may be suitable agents to keep the arginine side chain inside the LBP to activate W286R.

dx.doi.org/10.1021/jm400537h | J. Med. Chem. 2013, 56, 6745−6760

EXPERIMENTAL PROCEDURES

Protein Expression and Purification. To obtain the mutant VDR-LBD genes, we used QuikChange Site-Directed Mutagenesis Kit (Stratagene) and performed PCR with pET14b/rVDR-LBD plasmid[11b] as a template.

The rat VDR-LBDs (residues116–423 and Δ165–211) with or without the mutations were cloned as an N-terminal His6-tagged fusion protein into the pET14b expression vector and overexpressed in *Escherichia coli* C41, which is a modified strain from BL21. The cells were grown at 37 °C in LB medium (including ampicilin-Na 100 mg/L) and subsequently induced for 6 h with 15 μM isopropyl-β-D-thiogalactopyranoside (IPTG) at 23 °C. The purification procedure included affinity chromatography on a Ni-NTA column, followed by dialysis and ion-exchange chromatography (SP-sepharose). After tag removal by thrombin digestion, protease was removed by filtration through a HiTrap benzamidine column, and the protein was further purified by gel filtration on a Superdex200 column. The purity and homogeneity of the rVDR-LBD were assessed by SDS–PAGE.

Crystallization. Crystallization conditions for WT, R270L, and W282R have some difference. Purified WT solution was concentrated to about 0.75 mg/mL by ultrafiltration. To an aliquot (800 μL) of the protein solution was added each ligand (ca. 10 equivalents), the solution was further concentrated to attain about 100 μL, and then a solution (25 mM Tris-HCl, pH 8.0; 50 mM NaCl; 10 mM DTT; and 0.02% NaN_3) of coactivator peptide (H_2N-KNHPMLMNLLKDN-$CONH_2$, ca. 5 equivalents) derived from DRIP205 was added. These solutions of WT/ligands/peptide were allowed to crystallize by the vapor diffusion method using a series of precipitant solutions containing 0.1 M MOPS-NaOH (pH 7.0), 0.1–0.4 M sodium formate, 12–22% (w/v) PEG4000, and 5% (v/v) ethylene glycol.

Purified R270L solution was also concentrated to about 0.75 mg/mL by ultrafiltration. To an aliquot (800 μL) of the protein solution was added each ligand (ca. 10 or 20 equivalents), the solution was further concentrated to attain about 100 μL, and then the peptide solution was added. These solutions of R270L/ligands/peptide were allowed to crystallize using a series of precipitant solutions containing 0.1 M MOPS-NaOH (pH 7.0) (or 0.1 M Tris-HCl (pH 8.0), or 0.1 M glycine-NaOH (pH 9.0)), 0.4 M sodium formate, and 12–22% (w/v) PEG4000.

Purified W282R solution was concentrated to about 1.7 mg/mL by ultrafiltration. To an aliquot (350 μL) of the protein solution was added each ligand (ca. 10 or 20 equivalents), the solution was further concentrated to attain about 100 μL, and then the peptide solution was added. Solutions of W282R/natural hormone (**1**) or ligand **4a**/peptide were allowed to crystallize using a series of precipitant solutions containing 0.1 M MOPS-NaOH (pH 7.0), 0.05–0.2 M diammonium citrate, 14–26% (w/v) PEG4000, and 4% (v/v) 2-propanol. The other solution of W282R/ligand **4b**/peptide was allowed to crystallize using a series of precipitant solutions containing 0.1 M MOPS-NaOH (pH 7.0), 0.1 M sodium formate, 18–22% (w/v) PEG4000, and 5%(v/v) ethylene glycol.

Droplets for the crystallizations were prepared by mixing 2 μL of complex solution and 1 μL of precipitant solution, and droplets were equilibrated against 500 μL of precipitant solution at 20 °C. It took 1 to 3 days to obtain crystals with X-ray diffraction quality. The peptide derived from DRIP205 was essential for all of our crystallizations.

Diffraction Experiment and Structure Analysis. Prior to diffraction data collection, crystals were soaked in cryoprotectant solutions containing 17–20% ethylene glycol and the other reagents. Diffraction data sets were collected at 100 K in a stream of nitrogen gas at beamline BL-6A of KEK-PF and NW12A of PF-AR (Tsukuba, Japan). Reflections were recorded with an oscillation range per image of 1.0°. Diffraction data were indexed, integrated, and scaled using the program HKL2000.[25] The structures of complexes were solved by molecular replacement with the program CNS,[26] and finalized sets of atomic coordinates were obtained after iterative rounds of model modification with the program XtalView[27] and refinement with CNS by rigid body refinement, simulated annealing, positional minimization, water molecule identification, and individual isotropic B-value refinement.

Thermal Unfolding Measurement. Circular dichloism (CD) spectra were recorded on a Jasco J-820 spectropolarimeter at 20 °C in 10 mM Na-phosphate buffer (pH 7.0) containing 1 mM Tris 2-carboxyethyl phosphine (TCEP) and 1% ethanol. The samples analyzed in a 10 mm optical path length cell were 1 μM rVDR-LBD proteins in the absence or presence of 5 μM $1,25(OH)_2D_3$. CD spectra in the region of 200 to 250 nm were obtained using a scanning speed of 20 nm/min, a time response of 1 s, a bandwidth of 1 nm, a data interval of 0.2 nm, and an average of four scans. Thermal transition curves were determined by monitoring the CD values at 222 nm as the temperature was increased by 1.0 °C/min from 20 to 85 °C.

Luciferrase Assays. COS-7 cells were cultured in Dulbecco's modified Eagle's medium supplemented with 5% fetal calf serum. Cells were seeded on 24-well plates at a density of 2×10^4 per well. After 24 h, the cells were transfected with a reporter plasmid containing three copies of the mouse osteopontin VDRE (SPPx3-TK-Luc), a mutant hVDR expression plasmid [pCMX-hVDR], and the internal control plasmid containing sea pansy luciferase expression constructs (pRL-CMV) by the lipofection method as described previously.[28] After 4 h of incubation, the medium was replaced with fresh DMEM containing 5% charcoal-treated FCS (HyClone, UT, USA). The next day, the cells were treated with either the ligand or ethanol vehicle and cultured for 24 h. Cells in each well were harvested with a cell lysis buffer, and the luciferase activity was measured with a luciferase assay kit (Toyo Ink, Inc., Japan). Transactivation measured by luciferase activity was normalized with the internal control. All experiments were done in triplicate.

Synthesis of Ligands. *General.* All nonaqueous reactions were carried out under argon or nitrogen in freshly distilled anhydrous solvents. We conducted high-pressure liquid chromatography (HPLC) by using Jasco 880-PU pumps equipped with an 801-SC solvent programmer and a Uvidec-100 V variable-length UV–vis detector. All samples for biological assays were purified by HPLC and shown to have a purity of >95% [YMC-Pack ODS-AM SH-342–5, 15–20% H_2O/MeOH, 8 mL/min]. Nuclear magnetic resonance (^1H and ^{13}C) spectra were recorded in $CDCl_3$ solution on a Bruker ARX 400 MHz spectrometer. Low (MS)- and high-resolution mass spectra (HRMS) were obtained by electronic ionization (70 eV) on a JEOL JMS-AX505HA spectrometer. Ultraviolet spectra were recorded on a Hitachi U-3200 spectrophotometer.

*1α-(tert-Butyldimethylsilyloxy)-25-(methoxymethoxy)-19-norvitamin D_3 3-Pivaloyl Ester (**7**) and 1α-(Pivaloyloxy)-25-(methoxymethoxy)-19-norvitamin D_3 3-(tert-butyl dimethylsilyl) Ether (**8**).* A 1.0 M THF solution of LiHMDS (912 μL, 0.912 mmol) was added to a solution of arylsulphone **5** (486.8 mg, 0.912 mmol) in THF (3 mL) at −78 °C, and the mixture was stirred for 30 min. A solution of ketone **6** (228.8 mg, 0.696 mmol) in THF (3 mL) was added to the mixture at −78 °C, the mixture was stirred for 1 h, and then the temperature was raised to −40 °C for 2 h. Saturated NH_4Cl solution was added to the reaction, the mixture was extracted with AcOEt, and the organic layer was washed with brine, dried over $MgSO_4$, and evaporated. The residue was chromatographed on silica gel and eluted with 2–3% AcOEt/hexane to give **7** and **8** (334.8 mg, 74%) as a 2:1 mixture and with 10% AcOEt/hexane to give **5** (187.1 mg, 38%). A mixture (2:1) of **7** and **8**: ^1H NMR ($CDCl_3$) δ 0.07 (6 H, s, Si-Me × 2), 0.53, 0.50 (2: 1) (3 H, s, H-18), 0.88–0.89 (9 H, s, Si-*t*Bu), 0.92 (3 H, d, *J* = 6.4 Hz, H-21), 1.15, 1.14 (2: 1) (9 H, s, CO*t*Bu), 1.22 (6 H, s, H-26, 27), 3.37 (3 H, s, OCH_3), 3.96 (1 H, m), 4.71 (2 H, s, OCH_2O), 5.08, 5.15 (2: 1) (1 H, m), 5.82, 5.71 (2: 1) (1 H, d, *J* = 11.2 and 11.5 Hz, H-7), 6.15, 6.23 (2: 1) (1 H, d, *J* = 11.2 and 11.5 Hz, H-6). Mass *m/z* (%) 646 (M^+, 0.1), 584 (0.4), 544 (11), 482 (100).

*1α-(tert-Butyldimethylsilyloxy)-25-(methoxymethoxy)-19-norvitamin D_3 (**9**) and 1α-Hydroxy-25-(methoxymethoxy)-19-norvitamin D_3 3-(tert-Butyldimethylsilyl) Ether (**10**).* A solution of DIBALH (441 μL, 0.441 mmol, 1.01 M toluene solution) was added to a solution of **7** and **8** (2:1 mixture, 95.2 mg, 0.147 mmol) in toluene (1 mL) at −78 °C and stirred for 1.5 h. The reaction was quenched by adding saturated sodium potassium tartrate, and the mixture was

dx.doi.org/10.1021/jm400537h | J. Med. Chem. 2013, 56, 6745–6760

extracted with AcOEt, and the extract was washed with brine, dried over $MgSO_4$, and evaporated. The residue was chromatographed on silica gel (5 g) and eluted with 10% AcOEt/hexane to give a 2:1 mixture of **9** and **10** (71.7 mg, 87%). The mixture was further chromatographed on fine silica gel (C-300, 5 g) and eluted with 5% AcOEt/hexane to give **9** (25.2 mg), a mixture of **9** and **10** (21.8 mg), and then **10** (10.7 mg). **9**: ^{1}H NMR ($CDCl_3$) δ 0.06, 0.07 (each 3 H, s, Si-Me × 2), 0.54 (3 H, s, H-18), 0.88 (9 H, s, Si-*t*Bu), 0.93 (3 H, d, J = 6.4 Hz, H-21), 1.22 (6 H, s, H-26, 27), 2.14–2.24 (2 H, m, H-4, 10), 2.47 (1 H, dd, J = 13.1, 3.2 Hz, H-4), 2.56 (1 H, dd, J = 13.0, 3.5 Hz, H-10), 2.80 (1 H, dd, J = 12.5, 4.2 Hz, H-9), 3.37 (3 H, s, OCH_3), 4.00 (1 H, m, H-1), 4.12 (1 H, m, H-3), 4.71 (2 H, s, OCH_2O), 5.84 (1 H, d, J = 11.2 Hz, H-7), 6.25 (1 H, d, J = 11.2 Hz, H-6). MS m/z (%) 562 (M^+, 9), 544 (8), 500 (62), 482 (83), 443 (32), 425 (42), 350 (42), 75 (100). **10**: ^{1}H NMR ($CDCl_3$) δ 0.06, 0.07 (each 3 H, s, Si-Me × 2), 0.54 (3 H, s, H-18), 0.87 (9 H, s, Si-*t*Bu), 0.93 (3 H, d, J = 6.4 Hz, H-21), 1.22 (6 H, s, H-26, 27), 2.14 (1 H, dd, J = 12.7, 7.7 Hz, H-4), 2.39 (1 H, dd, J = 13.1, 4.2 Hz, H-4), 2.41 (2 H, m, H-10, OH), 2.80 (1 H, dd, J = 12.1, 3.6 Hz, H-9), 3.37 (3 H, s, OCH_3), 4.04 (1 H, m, H-3), 4.11 (1 H, m, H-1), 4.71 (2 H, s, OCH_2O), 5.82 (1 H, d, J = 11.1 Hz, H-7), 6.27 (1 H, d, J = 11.1 Hz, H-6). MS m/z (%) 562 (M^+, 13), 500 (77), 482 (80), 443 (27), 425 (35), 350 (35), 75 (100).

*1α-(tert-Butyldimethylsilyloxy)-25-(methoxymethoxy)-19-norvitamin D_3 3-Methoxymethyl Ether (**11a**).* To a solution of **9** (53.7 mg, 0.095 mmol) in CH_2Cl_2 (400 μL) at 0 °C were added ethyldiisopropylamine (50.1 μL, 0.286 mmol) and MOMCl (14.5 μL, 0.191 mmol), and the mixture was stirred at room temperature for 3 h. HCl solution (1 N) was added to the reaction mixture, the mixture was extracted with CH_2Cl_2, and the extract was washed with 5% $NaHCO_3$ and brine, dried over $MgSO_4$, and evaporated. The residue was chromatographed on silica gel (4 g) and eluted with 10% AcOEt/hexane to give **11a** (50.6 mg, 87%), and then **9** was recovered (6.0 mg, 11%). **11a**: ^{1}H NMR ($CDCl_3$) δ 0.06 (6 H, s, Si-Me × 2), 0.54 (3 H, s, H-18), 0.87 (9 H, s, Si-*t*Bu), 0.93 (3 H, d, J = 6.4 Hz, H-21), 1.22 (6 H, s, H-26, 27), 2.22 (1 H, dd, J = 14.2, 7.3 Hz, H-4), 2.32 (1 H, dd, J = 13.4, 6.8 Hz, H-10), 2.43 (2 H, m, H-4, 10), 2.80 (1 H, dd, J = 12.4, 3.9 Hz, H-9), 3.36, 3.37 (each 3 H, s, OCH_3), 3.96, 4.06 (each 1 H, m, H-1, 3), 4.66, 4.68 (each 1 H, s, OCH_2O), 4.71 (2 H, s, OCH_2O), 5.83 (1 H, d, J = 11.3 Hz, H-7), 6.23 (1 H, d, J = 11.3 Hz, H-6). MS m/z (%) 606 (M^+, 31), 576 (39), 544 (96), 482 (92), 73 (100).

*1α-Hydroxy-25-(methoxymethoxy)-19-norvitamin D_3 3-Methoxymethyl Ether (**11b**).* To a solution of **11a** (77.0 mg, 0.127 mmol) was added TBAF (380.6 μL, 0.381 mmol), and the mixture was stirred for 3 h at room temperature. Then additional TBAF (190.3 μL, 0.190 mmol) was added, and the mixture was stirred for 5.5 h. The mixture was extracted with AcOEt, and the extract was washed with brine, dried over $MgSO_4$, and evaporated. The residue was chromatographed on silica gel (3.5 g) and eluted with 30% AcOEt to give **11b** (59.4 mg, 95%). **11b**: ^{1}H NMR ($CDCl_3$) δ 0.54 (3 H, s, H-18), 0.93 (3 H, d, J = 6.4 Hz, H-21), 1.22 (6 H, s, H-26, 27), 2.27 (1 H, dd, J = 13.4, 7.1 Hz, H-4), 2.36 (1 H, dd, J = 13.5, 7.0 Hz, H-10), 2.47 (1 H, dd, J = 13.4, 3.7 Hz, H-4), 2.61 (1 H, dd, J = 13.5, 3.6 Hz, H-10), 2.80 (1 H, dd, J = 12.3, 4.0 Hz, H-9), 3.36, 3.37 (each 3 H, s, OCH_3), 3.96 (1 H, m, H-3), 4.10 (1 H, m, H-1), 4.666, 4.669 (each 1 H, s, OCH_2O), 4.71 (2 H, s, OCH_2O), 5.84 (1 H, d, J = 11.2 Hz, H-7), 6.31 (1 H, d, J = 11.2 Hz, H-6). MS m/z (%) 492 (M^+, 21), 462 (29), 430 (98), 400 (59), 368 (100), 350 (18).

*1α-{(2-tert-Butyldimethylsilyloxy)-ethyloxy}-25-(methoxymethoxy)-19-norvitamin D_3 3-Methoxymethyl Ether (**13**).* To a solution of **11b** (24.0 mg, 0.0487 mmol) in DMF (500 μL) at 0 °C were added NaH (60% in oil, 58.4 mg, 0.293 mmol) and then bromide **12** (70.0 mg, 0.293 mmol), and the mixture was stirred 15 h at room temperature. The reaction was quenched by adding ice water and extracted with 50% AcOEt/hexane. The extract was washed with brine, dried over $MgSO_4$, and evaporated. The residue was chromatographed on silica gel (4 g) and eluted with 6% AcOEt/hexane to give **13** (6.0 mg, 19%) and then eluted with 8% AcOEt/hexane to give **11b** (4.7 mg, 16%). **13**: ^{1}H NMR ($CDCl_3$) δ 0.07 (6 H, s, Si-Me × 2), 0.54 (3 H, s, H-18), 0.89 (9 H, s, Si-*t*Bu), 0.93 (3 H, d, J = 6.4 Hz, H-21), 1.22 (6 H, s, H-26, 27), 2.28 (1 H, dd, J = 13.6, 6.6 Hz, H-4), 2.35 (1 H, dd, J = 13.6, 7.5 Hz, H-10), 2.44 (1 H, dd, J = 13.6, 3.5 Hz, H-4), 2.60 (1 H, dd, J = 13.6, 3.4 Hz, H-10), 2.80 (1 H, dd, J = 12.2, 3.7 Hz, H-9), 3.36, 3.37 (each 3 H, s, OCH_3), 3.53 (2 H, m, OCH_2), 3.72 (3 H, m, H-1, OCH_2), 3.96 (1 H, m, H-3), 4.66, 4.71 (each 2 H, s, OCH_2O), 5.85 (1 H, d, J = 11.2 Hz, H-7), 6.23 (1 H, d, J = 11.2 Hz, H-6). MS m/z (%) 650 (M^+, 5), 588 (7), 526 (3), 73 (100).

*1α-(2-Hydroxyethoxy)-25-hydroxy-19-norvitamin D_3 (**2a**).* CSA (12.8 mg, 0.055 mmol) was added to a solution of **13** (6.0 mg, 9.2 μmol) in MeOH (700 μL), and the mixture was stirred for 2.5 h at room temperature. Additional CSA (12.8 mg, 0.055 mmol) was added and stirred for 20 h. 5% $NaHCO_3$ was added to the reaction, and the mixture was extracted with AcOEt. The extract was washed with brine, dried over $MgSO_4$, and evaporated. The residue was chromatographed on silica gel (3.5 g) and eluted with 1% MeOH/AcOEt to give **2a** (2.9 mg, 71%). **2a**: ^{1}H NMR ($CDCl_3$) δ 0.54 (3 H, s, H-18), 0.94 (3 H, d, J = 6.4 Hz, H-21), 1.22 (6 H, s, H-26, 27), 2.23 (2 H, m, H-4, 10), 2.49 (1 H, dd, J = 13.5, 3.0 Hz, H-4), 2.73 (1 H, dd, J = 13.2, 3.4 Hz, H-10), 2.80 (1 H, dd, J = 12.5, 4.1 Hz, H-9), 3.59, 3.70 (2 H, 3 H, m, H-1, OCH_2 × 2), 4.13 (1 H, m, H-3), 5.85 (1 H, d, J = 11.2 Hz, H-7), 6.26 (1 H, d, J = 11.2 Hz, H-6). MS m/z (%) 448 (M^+, 100), 430 (74), 412 (10). UV λ_{max} (EtOH) 244, 252, and 262 nm.

*1α-{4-tert-Butyldimethylsilyloxy)butoxy}-25-(methoxymethoxy)-19-norvitamin D_3 3-(tert-Butyldimethylsilyl) Ether (**15**).* NaH (60% in oil, 41.8 mg, 1.04 mmol) and then tosylate **14** (60.2 mg, 0.168 mmol) in dry DMF (300 μL) were added to a solution of **10b** (19.6 mg, 0.035 mmol) in DMF (500 μL) at 0 °C, and the mixture was stirred for 15 h. The reaction was quenched by ice water and extracted with 50% AcOEt/hexane, and the extract was washed with brine, dried over $MgSO_4$, and evaporated. The residue was chromatographed on silica gel (4 g) and eluted with 5% AcOEt/hexane to give **15** (20.6 mg, 79%). **15**: ^{1}H NMR ($CDCl_3$) δ 0.04, 0.05, 0.06 (3 H, 3 H, 6 H, s, Si-Me × 4), 0.54 (3 H, s, H-18), 0.87, 0.89 (each 9 H, s, Si-*t*Bu × 2), 0.93 (3 H, d, J = 6.5 Hz, H-21), 1.22 (6 H, s, H-26, 27), 2.80 (1 H, m, H-9), 3.37 (3 H, s, OCH_3), 3.42, 3.62 (2 H, 3 H, m, H-1, OCH_2 × 2), 4.05 (1 H, m, H-3), 4.71 (2 H, s, OCH_2O), 5.83 (1 H, d, J = 11.2 Hz, H-7), 6.16 (1 H, d, J = 11.2 Hz, H-6). MS m/z (%): 748 (M^+, 5), 686 (50), 554 (13), 482 (73), 73 (100).

*1α-(4-Hydroxybutoxy)-25-hydroxy-19nor-vitamin D_3 (**2b**).* CSA (38.3 mg, 0.165 mmol) was added to a solution of **15** (20.6 mg, 0.027 mmol) in MeOH (600 mL), and the mixture was stirred at room temperature for 1 h. 5% $NaHCO_3$ solution was added, and the mixture was extracted with AcOEt. The extract was washed with brine, dried over $MgSO_4$, and evaporated. The residue was chromatographed on silica gel (3 g) and eluted with 1% MeOH/AcOEt to give **2b** (12.9 mg, 99%). **2b**: ^{1}H NMR ($CDCl_3$) δ 0.55 (3 H, s, H-18), 0.94 (3 H, d, J = 6.4 Hz, H-21), 1.22 (6 H, s, H-26, 27), 2.20 (1 H, dd, J = 13.3, 6.1 Hz, H-4), 2.26 (1 H, dd, J = 13.3, 8.1 Hz, H-10), 2.48 (1 H, dd, J = 13.3, 3.1 Hz, H-4), 2.69 (1 H, dd, J = 13.3, 3.5 Hz, H-10), 2.80 (1 H, dd, J = 12.3, 3.9 Hz, H-9), 3.48, 3.54 (each 1 H, OCH_2), 3.63 (3 H, m, H-1, OCH_2), 4.11 (1 H, m, H-3), 5.85 (1 H, d, J = 11.2 Hz, H-7), 6.26 (1 H, d, J = 11.2 Hz, H-6). MS m/z (%): 476 (M^+, 19), 458 (23), 386 (100), 368 (74). UV λ_{max} (EtOH): 244 nm, 252 nm, 262 nm.

*1α-(tert-Butyldimethylsilyloxy)-25-methoxymethoxy-2-spiro-[oxirane]-19-norvitamin D_3 (**17**).* To a solution of sulphone **5** (159.7 mg, 0.299 mmol) in THF (1 mL) at −78 °C was added a 1.0 M THF solution of LiHMDS (299 μL, 0.299 mmol). The mixture was stirred for 30 min at −78 °C, and then a solution of A ring ketone **16** (67.3 mg, 0.174 mmol) in THF (1.5 mL) was added. The mixture was stirred at −78 °C for 1 h, and then the temperature was raised to −10 °C during 2.5 h. A saturated NH_4Cl solution was added to the reaction, the mixture was extracted with AcOEt, and the extract was washed with brine, dried over $MgSO_4$, and evaporated. The residue was chromatographed on silica gel (6 g) and eluted with 2–3% AcOEt/hexane to give **17** (88.7 mg, 72%) as a mixture of epimers at C(2) and recovered **7** (30.3 mg, 19%). **17**: ^{1}H NMR ($CDCl_3$) δ 0.02–0.08 (12 H, s, Si-Me × 4), 0.55 (3 H, s, H-18), 0.86, 0.88 (each 9 H, s, Si-*t*Bu × 2), 0.94 (3 H, d, J = 6.4 Hz, H-21), 1.22 (6 H, s, H-26, 27), 2.75 and 2.82, 2.57, and 2.92 (3:2) (each 1 H, d, J = 5.5 Hz, $-CH_2OC-$), 3.37 (3 H, s, OCH_3), 3.68 (minor) (1 H, dd, J = 4.9, 2.8 Hz, H-1 or −3), 3.81, 3.88 (major) (each 1 H, dd, J = 7.0, 3.8 Hz, H-1

dx.doi.org/10.1021/jm400537h | J. Med. Chem. 2013, 56, 6745–6760